metals

MDPI

Article

Effect of Microstructure on Fracture Toughness and Fatigue Crack Growth Behavior of Ti17 Alloy

Rong Liang [1], Yingping Ji [1,2,*], Shijie Wang [3] and Shuzhen Liu [1]

[1] College of Mechanical Engineering, Ningbo University of Technology, Ningbo 315211, China; mikesmile@163.com (R.L.); shuzhenl@163.com (S.L.)
[2] School of Materials Science and Engineering, Beihang University, Beijing 100191, China
[3] China National Heavy Machinery Research Institute Co., Ltd., Xi'an 710032, China; xzswangsj@163.com
* Correspondence: yingping04@163.com; Tel.: +86-574-8235-1508

Academic Editor: Soran Birosca
Received: 18 April 2016; Accepted: 20 July 2016; Published: 12 August 2016

Abstract: Ti-5Al-2Sn-2Zr-4Mo-4Cr (Ti17) is used extensively in turbine engines, where fracture toughness and fatigue crack growth (FCG) resistance are important properties. However, most research on the alloy was mainly focused on deformation behavior and microstructural evolution, and there have been few studies to examine the effect of microstructure on the properties. Accordingly, the present work studied the influences of the microstructure types (bimodal and lamellar) on the mechanical properties of Ti17 alloy, including fracture toughness, FCG resistance and tensile property. In addition, the fracture modes associated with different microstructures were also analyzed via the observation of the fracture surface. The results found that the lamellar microstructure had a much higher fracture toughness and superior resistance to FCG. These results were discussed in terms of the tortuous crack path and the intrinsic microstructural contributions.

Keywords: titanium alloys; microstructure; fracture toughness; fatigue crack growth behavior

1. Introduction

With the continuing desire to make engines with a high thrust-to-weight advantage, titanium alloys are the metals of choice for the gas turbine engine [1], where fracture toughness and resistance against fatigue failure are important properties. The optimized mechanical properties of titanium alloys can be achieved via controlling the microstructure. For example, Nalla et al. found that Ti-6Al-4V with a coarse lamellar microstructure had superior toughness while FCG (fatigue crack growth) behavior in large cracks was compared with a finer bimodal microstructure [2]. Verdhan et al. also found that Ti-6Al-2Zr-1.5Mo-1.5V with lamellar and acicular microstructures had lower FCG rates than that with the bimodal microstructure [3]. In general, three microstructures can be obtained in (α + β) and β titanium alloys: equiaxed, lamellar, and bimodal, which can be obtained by different thermomechanical processing [4]. The first is the result of a recrystallization process after minimal plastic deformation. The second one can be attained by an annealing process above the β-transus temperature (T_β) with subsequent cooling to the (α + β) phase. The third is the result of the annealing of a sufficiently plastically deformed (α + β) titanium alloy below the T_β [5].

As a replacement for the conventionally used α + β titanium alloys in high-strength airframe and jet engine structural parts, β titanium alloys have attracted a great deal of interest recently. Take Ti-5Al-2Sn-2Zr-4Mo-4Cr (Ti17), for example: due to its higher strength level as compared to the typical α + β Ti-6Al-4V alloy [6–8], the alloy has been favored as a jet engine compressor and has attracted more attention in recent times [6–16]. Luo et al. conducted isothermal compression tests on Ti17 alloy and observed the microstructural evolution [11]. Wang et al. studied the grain growth kinetics of Ti17 alloys in the β phase [12]. Teixeira et al. investigated the transformation kinetics and

microstructural evolution of Ti17 titanium alloy during continuous cooling [13]. Tarín et al. assessed the ultimate tensile strength, yield strength and elongation of Ti17 alloy [14]. Xu et al. studied the effect of globularization behavior of the lamellar alpha on the tensile properties of Ti17 alloy and found that there are linear relationships between tensile properties and the globularization fraction [15]. Moshier et al. investigated the load history effects on the fatigue crack growth threshold of Ti17 alloy [16]. Shi et al. studied the effects of lamellar features on the fracture toughness of Ti17 titanium alloy and found that the microstructure with long and thick needle-like α platelets had higher fracture toughness and strength than that with short rod-like α platelets [9]. It can be found that the previous research on Ti17 alloy was mainly focused on deformation behavior and microstructural evolution. However, there have been few studies to examine the effects of microstructure on fracture toughness and FCG behavior.

Thus, in this paper, the influences of the microstructural types (bimodal and lamellar) on the mechanical properties of Ti17 alloy were investigated, including yield stress, ductility, and fracture toughness as well as FCG properties. To investigate the fracture mode, the fracture surfaces of specimens after tests were observed by scanning electron microscopy (SEM).

2. Materials and Methods

The material used in this study is Ti17 alloy, whose chemical composition is detailed in Table 1.

Table 1. Chemical composition of Ti17 (wt. %).

Element	Al	Sn	Zr	Mo	Cr	Fe	C	N	H	O	Ti
wt. %	5.01	1.98	2.02	4.15	4.33	0.30	0.05	0.05	0.0125	0.09	Balance

To obtain two different microstructures of interest, materials were subjected to α + β and β processing route respectively. In α + β process, Ti17 alloys as received condition were hot forged in the α + β phase field at 850 °C, followed by air cooling to room temperature. Subsequently, the materials were recrystallized in the α + β phase field at 870 °C for 1 h to adjust a low volume fraction of the primary α phase (α_p), followed by air cooling to room temperature. Finally, materials were aged 8 h at 580 °C to precipitate fine secondary α (α_s). In β process, as received materials were first α + β forged at 850 °C and then heated to 920 °C into the β phase field to coarsen the β grain structure for 1 h, followed by air cooling. At last, these materials were aged at 580 °C for 8 h to precipitate α_s. The microstructures of the α + β and β processed were observed by SEM on an Apollo 300 (Camscan, Cambridge, UK) and they are illustrated in Figure 1. It is obvious that the material of the α + β processed exhibits the bimodal microstructure, and that β processed yields the lamellar one.

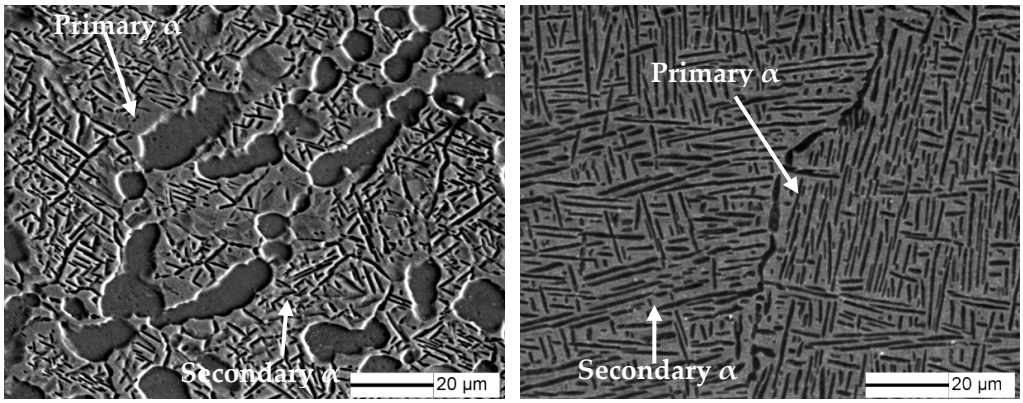

(**a**) (**b**)

Figure 1. Microstructure of Ti17: (**a**) bimodal; (**b**) lamellar.

The quasi-static tensile tests were conducted at room temperature and in the laboratory air environment using a fully automated, closed-loop servo-hydraulic machine (INSTRON 8801). The specimens were made of a dog-bone shape (Figure 2a) and deformed to failure at a constant strain rate of 10^{-3}·s^{-1}. These tests yielded basic mechanical properties such as yield strength, tensile strength and ductility.

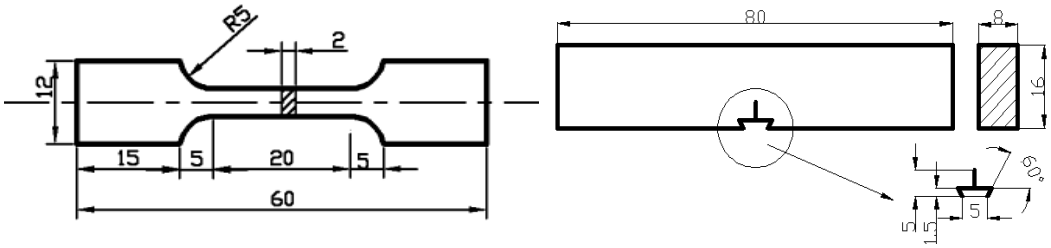

(**a**) (**b**)

Figure 2. Specimens for (**a**) tensile; (**b**) fracture toughness and fatigue crack growth tests.

Fatigue and fracture toughness measurements were also carried out using the servo-hydraulic testing machine INSTRON 8801 and performed at room temperature. Mode I fracture toughness tests were performed using three-point (3P) bending specimens, with the geometry as described in Figure 2b. The specimens were loaded according to the standard three-point bending method gripped all along their width and fatigue precracks were initiated to a depth of 8 mm. Subsequently, monotonic loading was applied to the specimen until the crack propagated catastrophically to fracture. Further calculation details of fracture toughness were according to the BS7448-1:1991 standards. Fatigue crack growth experiments were conducted on the same specimens, in according with ASTM E647-93 standard. FCG experiments were carried out on with a frequency of 6 Hz under constants tress ratio R = 0.1 and the fatigue crack length (a) was monitored using compliance method.

For a given variant, three specimens were tested and the average values of the mechanical properties were determined. In addition to mechanical testing, the fracture surfaces of the failed specimens with different microstructures were examined by SEM to determine the macroscopic fracture mode and mechanisms.

3. Results and Discussion

3.1. Tensile Properties

The average values of the tensile properties of the tested specimens are summarized in Table 2, including yield strength (YS), ultimate tensile strength (US) and percentage elongation (A%). The values listed are an average of three tests. It can be found that the bimodal microstructure has a slightly increasing strength and higher plasticity than the lamellar one, indicative of a comparable tensile strength and a higher ductility of the former. The tensile ductility of α-β titanium alloys is mainly determined by two parameters, crack nucleation resistance and crack propagation resistance, and the former is the dominating parameter. Gungor et al. pointed out that colony boundaries and α at prior β grain boundaries served as void nucleation sites [17]. Thus, the increasing volume of α_p phases in the bimodal microstructure decreased the slip length and initiated more sites of void nucleation, leading to the higher ductility.

Table 2. Mechanical properties of Ti17 alloy with bimodal and lamellar structure.

Specimens	US/MPa	YS/MPa	A/%	CTOD/μm
Bimodal structure	1220	1165	13	12
Lamellar structure	1205	1150	9.8	68

Representative fractographs of the tensile specimens are shown in Figure 3, which reveal the specific role played by the microstructural effects on strength and ductility properties. As Figure 3a depicted, some randomly distributed ductile dimples in globular shapes cover the transgranular fracture regions, suggesting locally ductile failure occurred in the bimodal microstructure. In the case of the lamellar microstructure, the fracture surface was similar to the counterpart of the bimodal microstructure, i.e., some elongated dimples in the center of Figure 3b could also be noted. However, the dimples were smaller than in the former, corresponding to the lower value of percentage elongation. Assisting with the features observation of the fracture surfaces, it can be concluded that the ductile failure mechanism governed the tensile response of Ti17 alloy with both bimodal and lamellar microstructures.

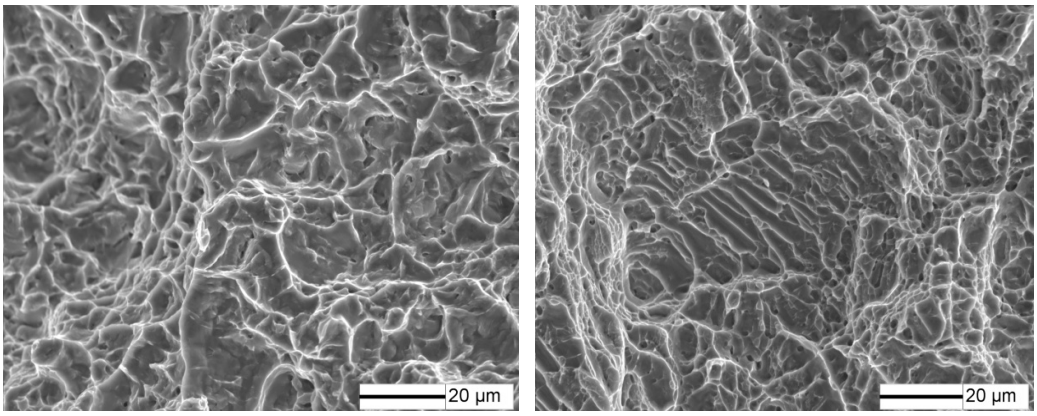

(**a**) (**b**)

Figure 3. Tensile fracture surfaces of Ti17: (**a**) bimodal; (**b**) lamellar.

3.2. Fracture Toughness

A preliminary calculation revealed that, for the specimen size considered in these investigations, a valid plane strain fracture toughness, K_{IC}, could not be obtained. Hence, the crack tip opening displacement (CTOD), at the onset of crack initiation, was chosen as the critical fracture toughness of specimens. The average CTOD values were also enumerated in Table 2 and each value listed is an average of three tests. It can be observed that the lamellar microstructure exhibits higher fracture toughness as compared with the bimodal microstructure. Therefore, from the point of the damage tolerance design concept, titanium alloy with a lamellar microstructure is more significant than that with a bimodal microstructure, which is in agreement with the previous report [18].

Representative SEM micrographs depicting the fracture surfaces of bimodal and lamellar microstructures are shown in Figure 4. It is evident that fracture surfaces of both were covered with dense dimples. Crack propagated in ductile mode, which was also found in Reference [7]. However, some big differences between the two microstructures were observed. On one hand, the dimples on the fracture surfaces shown in Figure 4a are obviously bigger and deeper than those shown in Figure 4b. This indicates that the bimodal microstructure has higher plasticity than the lamellar microstructure, which is consistent with the tensile results shown in Table 2. On the other hand, the fracture surface of the lamellar microstructure is characterized by secondary cracks and a big fracture step, which increases the toughness.

Previous investigations found that there was a positive correlation between the crack path length and the fracture toughness [7,19,20]. Therefore, the crack path geometry has to be taken into account as a parameter responsible for the different fracture toughness. As depicted in Figure 5 (the nominal crack propagation direction is indicated by the arrow), bimodal and lamellar microstructures both fractured in tortuous paths during the fracture process, but the lamellar microstructure displays a more tortuous and deflected crack path than the former. Such increased crack-path tortuosity is a major contributor to

the higher toughness of the lamellar microstructure. The tortuous and deflected crack path consumed much more energy than the flat one, leading to the higher fracture toughness. Cracks grew along a more tortuous and deflected crack path in lamellar microstructures, which over-compensated the lower ductility, resulting in the higher fracture toughness. The tortuous and deflected crack path was related with the more discontinuous α precipitates at the grain boundary. Therefore, it can be concluded that the long and thick α platelets in the lamellar microstructure can realize a good combination of fracture toughness and strength.

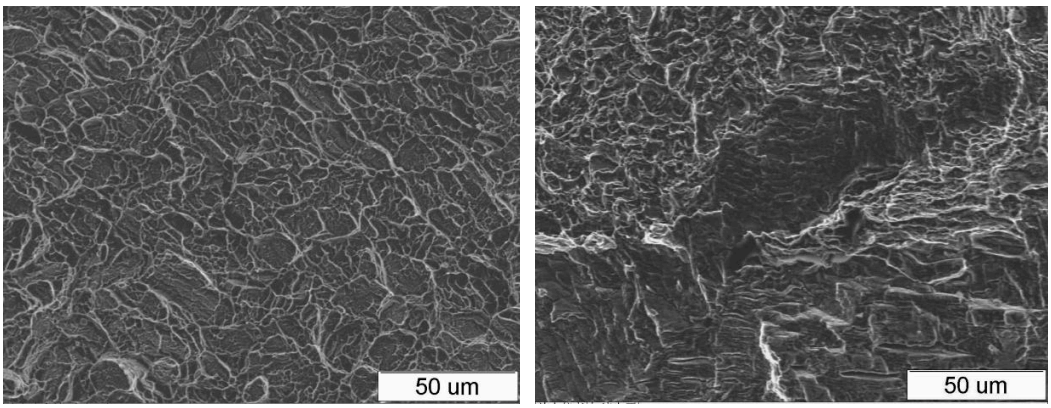

(**a**) (**b**)

Figure 4. Fracture surfaces of specimens for fracture toughness test: (**a**) bimodal; (**b**) lamellar.

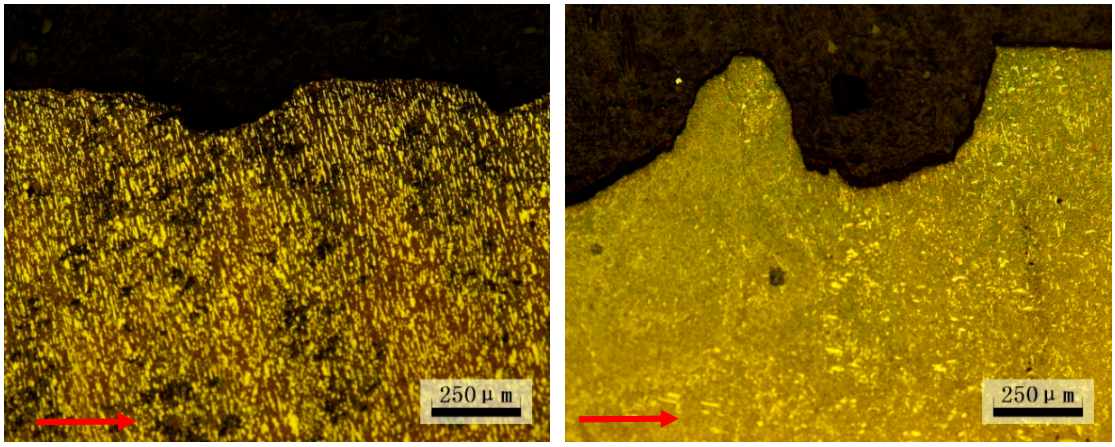

(**a**) (**b**)

Figure 5. Metallographic profile of the crack path in Ti17: (**a**) bimodal; (**b**) lamellar.

3.3. Fatigue Crack Growth Behavior

The variation in FCG rates in bimodal and lamellar microstructures is presented in Figure 6. The fracture mechanics based on the Paris Power equation, given below, were used to analyze the experimental results.

$$da/dN = C(\Delta K)^m \quad (1)$$

where da/dN is the FCG rate, ΔK is the stress intensity factor range, and the exponent "m" and coefficient "C" are the slope and the intercept of the line on the log-log plot respectively, and both are constant.

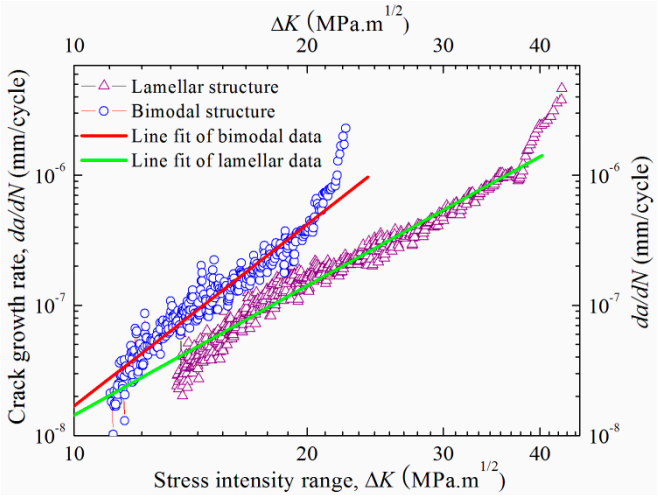

Figure 6. FCG behavior of bimodal and lamellar microstructures.

The Paris Power law relations (in units of mm/cycle, $MPam^{1/2}$) of bimodal and lamellar microstructures are shown as follows.

$$\frac{da}{dN} = 1.54 \times 10^{-8} \times (\Delta K)^{4.63} (\text{Bimodal structure}) \quad (2)$$

$$\frac{da}{dN} = 1.14 \times 10^{-8} \times (\Delta K)^{3.44} (\text{Lamellar structure}) \quad (3)$$

Although the differences are not large, in the lamellar structure, FCG rates (da/dN) were consistently lower and the threshold is higher than that in the bimodal microstructure. Thus, the lamellar structure clearly provides superior FCG resistance compared to the bimodal structure, which can primarily be traced to the increased tortuosity in the crack path in the lamellar structure. As shown in Figure 7, the crack path in the bimodal microstructure is straight, but it appears more deflected in the lamellar microstructure (the nominal crack propagation direction is indicated by the arrow).

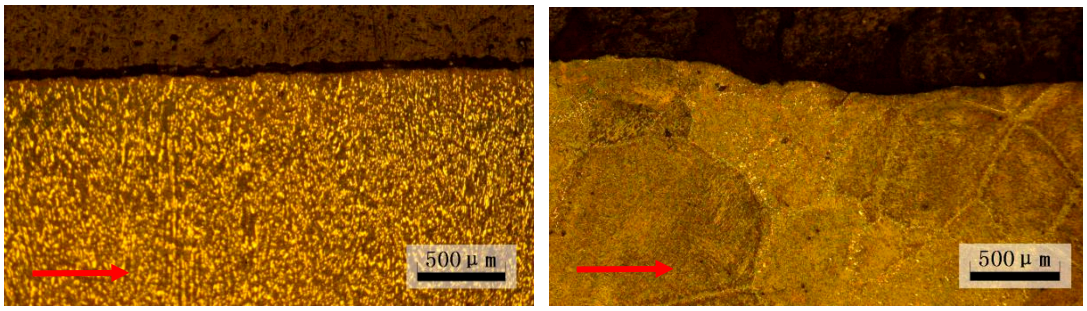

(**a**) (**b**)

Figure 7. A typical crack profile observed for the (**a**) bimodal and (**b**) lamellar microstructure.

The tortuous crack path in the lamellar structure resulted in a far rougher fracture surface, as shown by the SEM in Figure 8a,b for bimodal and lamellar structures, respectively. Typical fatigue striations and secondary cracks were observed on both fracture surfaces. However, the fracture surface of the lamellar microstructure is much rougher than that of the bimodal microstructure. In addition, there are more microscopic cracks detected in Figure 8b. Due to the tortuous nature of the cracks, the lamellar microstructure had a higher FCG resistance than the bimodal microstructure, which was also observed in the FCG behavior of a near-α Ti alloy [3].

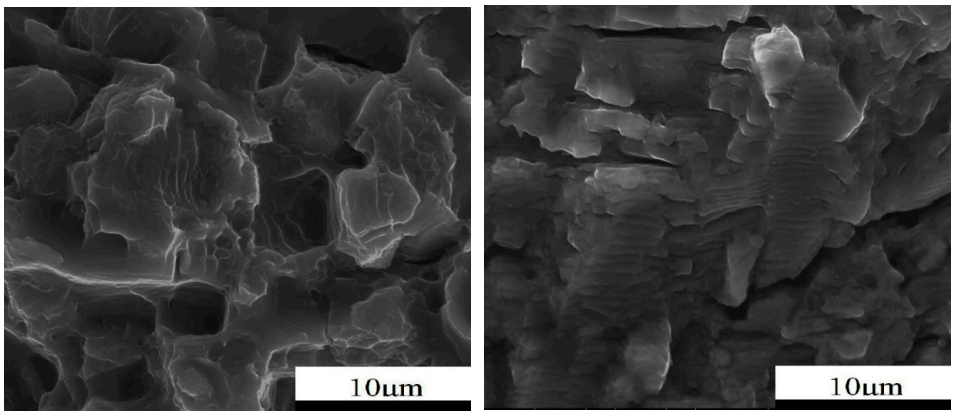

(**a**) (**b**)

Figure 8. Fracture topography of Ti17 in Regime II of FCG: (**a**) bimodal; (**b**) lamellar.

The different damage modes are consistent with the microstructures. As Nalla et al. found, the crack paths in titanium alloys were strongly influenced by the orientation of neighboring colonies [2]. In the present study, the lamellar microstructure had big colonies of lath α and β, which acted as an effective slip barrier to prevent the transmission of slip to neighboring colonies. The cracks changed direction when they crossed the boundary between colonies. Thus, they caused crack branching and secondary crack creation. The occurrence of secondary cracking effectively reduced the local crack tip driving force due to the redistribution of stresses [21], resulting in the lower FCG rates of the lamellar microstructure. In the case of the bimodal microstructure, there were no obvious colonies and the fatigue crack grew in a straight way, resulting in a relatively higher FCG rate than the lamellar microstructure.

4. Conclusions

Based on the study of the mechanical properties of Ti17 alloys with bimodal and lamellar microstructure, the following conclusions can be made:

(1) The lamellar microstructure showed a superior fracture toughness over the bimodal structure, which was associated with the intrinsic microstructural contributions and tortuous crack path.

(2) The lamellar microstructure had a higher threshold stress intensity factor and a greater FCG resistance than the bimodal microstructure.

Acknowledgments: This work has been financially supported by "Fracture Mechanism of Dissimilar Titanium Alloy Welded Joints" Ningbo Natural Science Foundation program (NO.2015A610071) and the Zhejiang Natural Science Foundation program (NO.LQ13E050005). As part of these grants, we received funds for covering the costs to publish in open access.

Author Contributions: Rong Liang and Yingping Ji conceived and designed the experiments; Yingping Ji performed the experiments, analyzed the data and wrote the manuscript; Shijie Wang and Shunzhen Liu contributed to editing the manuscript.

Conflicts of Interest: The authors declare no conflict of interest.

Abbreviations

The following abbreviations are used in this manuscript:

α	Hexagonal phase in titanium alloys
β	Body-centered cubic phase in titanium alloys
T_β	Beta-transus temperature
a	Crack length
C, m	Parameters of the Paris-Erdogan equation
$\mathrm{d}a/\mathrm{d}N$	Fatigue crack growth rate
ΔK	Cyclic stress intensity factor
N	Number of cycles

References

1. Elrod, C.W. Review of Titanium Application in Gas Turbine Engines. In Proceedings of the ASME Turbo Expo 2003, collocated with the 2003 International Joint Power Generation Conference, Atlanta, GA, USA, 16–19 June 2003; pp. 649–656.
2. Nalla, R.K.; Boyce, B.L.; Campbell, J.P.; Peters, J.O.; Ritchie, R.O. Influence of Microstructure on High-Cycle Fatigue of Ti-6Al-4V: Bimodal vs. Lamellar Structures. *Metall. Mater. Trans. A* **2002**, *33*, 899–917. [CrossRef]
3. Verdhan, N.; Bhende, D.D.; Kapoor, R.; Chakravartty, J.K. Effect of microstructure on the fatigue crack growth behaviour of a near-α Ti alloy. *Int. J. Fatigue* **2015**, *74*, 46–54. [CrossRef]
4. Lütjering, G. Influence of processing on microstructure and mechanical properties of (α + β) titanium alloys. *Mater. Sci. Eng. A* **1998**, *243*, 32–45. [CrossRef]
5. Krüger, L.; Grundmann, N.; Trubitz, P. Influence of Microstructure and Stress Ratio on Fatigue Crack Growth in a Ti-6-22-22-S alloy. *Mater. Today Proc.* **2015**, *2*, 205–211. [CrossRef]
6. Li, W.Y.; Ma, T.; Yang, S. Microstructure Evolution and Mechanical Properties of Linear Friction Welded Ti-5Al-2Sn-2Zr-4Mo-4Cr (Ti17) Titanium Alloy Joints. *Adv. Eng. Mater.* **2010**, *12*, 35–43. [CrossRef]
7. Shi, X.H.; Zeng, W.D.; Zhao, Q.Y. The effects of lamellar features on the fracture toughness of Ti17 titanium alloy. *Mater. Sci. Eng. A* **2015**, *636*, 543–550. [CrossRef]
8. Cadario, A.; Alfredsson, B. Fatigue growth of short cracks in Ti17: Experiments and simulations. *Eng. Fract. Mech.* **2007**, *74*, 2293–2310. [CrossRef]
9. García, A.M.M. *BLISK Fabrication by Linear Friction Welding*; INTECH Open Access Publisher: Rijeka, Croatia, 2011.
10. Kumar, B.V.R.R. A Review on Blisk Technology. *Int. J. Innov. Res. Sci. Eng. Technol.* **2013**, *2*, 1353–1358.
11. Luo, J.; Li, L.; Li, M.Q. The flow behavior and processing maps during the isothermal compression of Ti17 alloy. *Mater. Sci. Eng. A* **2014**, *606*, 165–174. [CrossRef]
12. Wang, T.; Guo, H.Z.; Tan, L.J.; Yao, Z.K.; Zhao, Y.; Liu, P.H. Beta grain growth behaviour of TG6 and Ti17 titanium alloys. *Mater. Sci. Eng. A* **2011**, *528*, 6375–6380. [CrossRef]
13. Teixeira, J.D.C.; Appolaire, B.; Aeby-Gautier, E.; Denis, S.; Cailletaud, G.; Späth, N. Transformation kinetics and microstructures of Ti17 titanium alloy during continuous cooling. *Mater. Sci. Eng. A* **2007**, *448*, 135–145. [CrossRef]
14. Tarín, P.; Fernández, A.L.; Simón, A.G.; Badía, J.M.; Piris, N.M. Transformations in the Ti-5Al-2Sn-2Zr-4Mo-4Cr (Ti-17) alloy and mechanical and microstructural characteristics. *Mater. Sci. Eng. A* **2006**, *438–440*, 364–368. [CrossRef]
15. Xu, J.W.; Zeng, W.D.; Zhao, Y.W.; Jia, Z.Q.; Sun, X. Effect of globularization behavior of the lamellar alpha on tensile properties of Ti-17 alloy. *J. Alloy. Compd.* **2016**, *673*, 86–92. [CrossRef]
16. Moshier, M.A.; Nicholas, T.; Hillberry, B.M. Load history effects on fatigue crack growth threshold for Ti-6Al-4V and Ti-17 titanium alloys. *Int. J. Fatigue* **2001**, *23*, 253–258. [CrossRef]
17. Gungor, M.N.; Ucok, I.; Kramer, L.S.; Dong, H.; Martin, N.R.; Tack, W.T. Microstructure and mechanical properties of highly deformed Ti-6Al-4V. *Mater. Sci. Eng. A* **2005**, *410–411*, 369–374. [CrossRef]
18. Chandravanshi, V.K.; Bhattacharjee, A.; Kamat, S.V.; Nandy, T.K. Influence of thermomechanical processing and heat treatment on microstructure, tensile properties and fracture toughness of Ti-1100-0.1B alloy. *J. Alloy. Compd.* **2014**, *589*, 336–345. [CrossRef]
19. Xue, Y.L.; Li, S.M.; Zhong, H.; Fu, H.Z. Characterization of fracture toughness and toughening mechanisms in Laves phase Cr_2Nb based alloys. *Mater. Sci. Eng. A* **2015**, *638*, 340–347. [CrossRef]
20. Shi, X.H.; Zeng, W.D.; Zhao, Q.Y. The effect of surface oxidation behavior on the fracture toughness of Ti-5Al-5Mo-5V-1Cr-1Fe titanium alloy. *J. Alloy. Compd.* **2015**, *647*, 740–749. [CrossRef]
21. Stephens, R.R.; Stephenst, R.I.; Veitt, A.L.; Albertson, T.P. Fatigue crack growth of Ti-62222 titanium alloy under constant amplitude and minitwist flight spectra at 25 °C and 175 °C. *Int. J. Fatigue* **1997**, *19*, 301–308. [CrossRef]